PHYSICAL REVIEW D **71,** 094501 (2005)

Testing improved staggered fermions with m_s and B_K

Weonjong Lee,[1,*] Tanmoy Bhattacharya,[2,†] George T. Fleming,[3,‡] Rajan Gupta,[2,§] Gregory Kilcup,[4,‖] and Stephen R. Sharpe[5,¶]

[1]*School of Physics, Seoul National University, Seoul, 151-747, Republic of Korea*
[2]*Los Alamos National Laboratory, MS–B285, T-8, Los Alamos, New Mexico 87545, USA*
[3]*Jefferson Laboratory, 12000 Jefferson Avenue, Newport News, Virginia 23606, USA*
[4]*Department of Physics, The Ohio State University, Columbus, Ohio 43210, USA*
[5]*Physics Department, University of Washington, Seattle, Washington 98195-1560, USA*

(Received 14 September 2004; revised manuscript received 17 February 2005; published 2 May 2005)

We study the improvement of staggered fermions using hypercubically smeared links. We calculate the strange quark mass and the kaon B parameter, B_K, in quenched QCD on a $16^3 \times 64$ lattice at $\beta = 6.0$. We find $m_s(\overline{\mathrm{MS}}, 2\ \mathrm{GeV}) = 101.2 \pm 1.3 \pm 4$ MeV and $B_K(\overline{\mathrm{MS}}, 2\ \mathrm{GeV}) = 0.578 \pm 0.018 \pm 0.042$, where the first error is from statistics and fitting, and the second from using one-loop matching factors. The scale ($1/a = 1.95$ GeV) is set by M_ρ, and m_s is determined using the kaon mass. Comparing to quenched results obtained using unimproved staggered fermions and other discretizations, we argue that the size of discretization errors in B_K is substantially reduced by improvement.

DOI: 10.1103/PhysRevD.71.094501 PACS numbers: 11.15.Ha, 12.38.Aw, 12.38.Gc

I. INTRODUCTION

One of the major sources of uncertainty in using precision experimental data to constrain the standard model is the lack of knowledge of the matrix elements of the effective weak Hamiltonian between hadronic states. The kaon bag parameter B_K, which parametrizes the matrix element of the $\Delta S = 2$ operator responsible for kaon-antikaon mixing, is one such key input for the determination of the Cabibbo-Kobayashi-Maskawa mixing matrix. It is defined as the dimensionless ratio

$$B_K = \frac{\langle \bar{K}^0 | \bar{s}\gamma_\mu(1-\gamma_5)d\bar{s}\gamma_\mu(1-\gamma_5)d|K^0\rangle}{\frac{8}{3}\langle \bar{K}^0|\bar{s}\gamma_\mu\gamma_5 d|0\rangle\langle 0|\bar{s}\gamma_\mu\gamma_5 d|K^0\rangle}. \quad (1)$$

Different approaches, including chiral perturbation theory, the large N_c expansion, QCD sum rules and lattice QCD, have been used to estimate B_K. The advantage of the lattice approach is that it is a first principle, nonperturbative determination. On the other hand it introduces statistical and systematic errors like those due to discretization and the matching of lattice and continuum operators. To gain control over these uncertainties, different fermion discretizations—Wilson, staggered, domain wall and overlap—have been used in simulations.[1]

In this note we explore the extent to which improved staggered fermions can be used to reduce two of the most important systematic errors, i.e., those due to discretization and the matching of lattice and continuum operators. This test is carried out in the quenched approximation to get an estimate of the size of these errors by comparing with existing data. Our ultimate aim, however, is to find a method which can be used effectively on dynamical lattices likely to be produced in the near future.

Staggered fermions are an attractive choice for the calculation of weak matrix elements because they are computationally efficient—indeed, simulations with three dynamical flavors are already possible with relatively light quark masses [2]—and yet retain sufficient chiral symmetry to protect operators of physical interest from mixing with others of wrong chirality. Their disadvantage is that they retain four "tastes" of doublers for each lattice field. In the continuum limit, these four tastes become degenerate, and one can remove the additional degrees of freedom by hand. For the valence quarks this procedure is explained for the calculation of B_K in Ref. [3], while for the sea quarks one must take the fourth root of the quark determinant. At nonzero lattice spacing, however, quark-gluon interactions violate the taste symmetry. This has three important consequences for calculations of B_K.

The first concerns taste-symmetry violation and the need to take the fourth root of the quark determinant. For nonzero lattice spacing, there is no proof that the underlying lattice action is local and lies in the same universality class as QCD. Even though we do not face this problem in quenched simulations, it is relevant when extending our calculations to dynamical simulations. Our justification for proceeding is empirical— accurate unquenched simulations using the fourth root of the determinant find agreement between lattice and experimental results [2].

Second, large $\mathcal{O}(a^2)$ discretization errors have been observed in the calculation of masses and matrix elements. Overcoming these requires the use of very small lattice spacings to make reliable continuum extrapolations. Last, many one-loop perturbative estimates of matching factors

*Electronic address: wlee@phya.snu.ac.kr
†Electronic address: tanmoy@lanl.gov
‡Electronic address: flemingg@jlab.org
§Electronic address: rajan@lanl.gov
‖Electronic address: kilcup@physics.ohio-state.edu
¶Electronic address: sharpe@phys.washington.edu
[1]See Ref. [1] for a recent review.

differ significantly from their tree-level value of unity, raising doubts about their accuracy [4].

The purpose of this paper is to show, using m_s and B_K as probes, that the latter two problems can be greatly alleviated by improving staggered fermions using "fat" links [5]. Based on the analysis of Ref. [6], we choose a particular type of fattening, hypercubic (HYP) smeared links [7], although we expect that other choices will work comparably well. Earlier calculations show that taste-symmetry violations in the spectrum are substantially reduced [7,8], and one-loop corrections to matching factors for four-fermion operators which were as large as 100% are now reduced to ~10% [9]. The largest improvement is in renormalization constants of left-right (penguin) four-fermion operators [9], and this can be traced back to the improvement in $Z_m = 1/Z_S = 1/Z_P \approx 1$ with HYP smearing. This has a major impact on the extraction of m_s as we show in Sec. III. In the case of B_K the major impact of improvement is to reduce discretization errors. This is because the one-loop corrections to matching factors in this case turn out to be small ($\sim 10\%$) before (as well as after) improvement.

To test the efficacy of improvement for m_s and B_K, we compare our results to the JLQCD analyses with unimproved staggered fermions that include detailed studies of both discretization and perturbative errors [10,11].

This paper is organized as follows. In Sec. II, we analyze the ρ meson spectrum calculated on the HYP smeared lattices and obtain the lattice scale $1/a$. In Sec. III, we present the extraction of the strange quark mass from the pion spectrum and compare the result with that obtained using unimproved staggered fermions. In Sec. IV, we present results for B_K calculated using the HYP improved staggered fermions and compare them with those of unimproved staggered fermions and with some recent data obtained using domain wall and overlap fermion formulations. We close with some conclusions in Sec. V.

II. ρ MESON SPECTRUM

The statistical sample consists of an ensemble of 218 gauge configurations of size $16^3 \times 64$ generated using the Wilson plaquette action at $\beta = 6.0$. The lattices were first HYP smeared using the tree-level improved parameters of Ref. [6]. On these HYP smeared lattices quark propagators are calculated using $2Z$ wall sources on time slices 0, 16, 32 and 48 for the bare quark masses listed in Table I.[2] Meson correlators are calculated at all time slices for each set of the $2Z$ wall sources. Throughout this work we only consider mesons composed of degenerate quarks.

The lattice scale is set using the ρ meson mass. We calculated correlators for two types of ρ mesons: $\rho(1)$, with spin taste $(\gamma_i \otimes \xi_i)$; and $\rho(2)$, with spin taste $(\gamma_i\gamma_4 \otimes \xi_i\xi_4)$. The correlators are fit to the standard form [13]:

[2]The details on the $2Z$ wall source are given in Ref. [12].

TABLE I. Quark masses used in simulation and their relation to the strange quark mass.

Name	am_q	m_q/m_s
m_1	0.01	0.192
m_2	0.02	0.385
m_3	0.03	0.577
m_4	0.04	0.769

TABLE II. Masses of ρ and a_1 mesons, and resulting scales.

m_q	$aM_\rho(\gamma_i \otimes \xi_i)$	$aM_\rho(\gamma_i\gamma_4 \otimes \xi_i\xi_4)$	$aM_{a_1}(\gamma_i\gamma_5 \otimes \xi_i\xi_5)$
m_1	...	0.4244(63)	0.5897(345)
m_2	0.4444(32)	0.4466(40)	0.6350(218)
m_3	0.4676(32)	0.4692(43)	0.6387(347)
m_4	0.4865(25)	0.4879(32)	0.6657(250)
$1/a$	...	1945(50) MeV	2112(131) MeV

$$C(t) = Z_1\{\exp[-m_1 t] + \exp[-m_1(L-t)]\} + Z_2(-1)^t \times \{\exp[-m_2 t] + \exp[-m_2(L-t)]\} \quad (2)$$

where m_1 is the mass of the ρ meson, while m_2 is the mass of its opposite parity partner, whose contribution has an alternating sign in the time direction. The partner for $\rho(1)$ is the b_1 meson, with spin taste $(\gamma_j\gamma_k \otimes \xi_j\xi_k)$, while that for the $\rho(2)$ is the a_1 with spin taste $(\gamma_i\gamma_5 \otimes \xi_i\xi_5)$.

We obtain good fits to both ρ correlators except for the $\rho(1)$ at the lightest quark mass. The resulting masses, as well as those of the parity partner a_1, are given in Table II. Since we want to be able to use all four quark masses to carry out the chiral extrapolation, we opt to consider only the $\rho(2)$ results to determine the lattice scale. We do not, however, expect that the resulting scale would change significantly were we to use $\rho(1)$ masses, because the $\rho(1)$ and $\rho(2)$ masses agree within errors for the three heavier quark masses. To illustrate the quality of the fits we show the effective mass plots for $\rho(2)$ as a function of time in Figs. 1–4. The effective mass at time $t = T$ is defined to be the value of m_1 obtained by solving Eq. (2) using the correlation function on time slices T to $T + 3$. All errors are determined using single elimination jackknife, with the underlying fits (both in t and m) using uncorrelated errors, because the correlation matrix is determined with insufficient accuracy.

The result of a quadratic fit to $M_{\rho(2)}$ versus quark mass, shown in Fig. 5, is

$$aM_\rho = 0.399(10) + 2.60(59)(am_q) - 9.3(8.7)(am_q)^2. \quad (3)$$

From this we estimate the lattice scale $1/a$ quoted in Table II by setting the chirally extrapolated value $0.399(10) = aM_\rho^{\text{physical}}$. The change in the resulting scale from extrapolating to the physical light quark masses

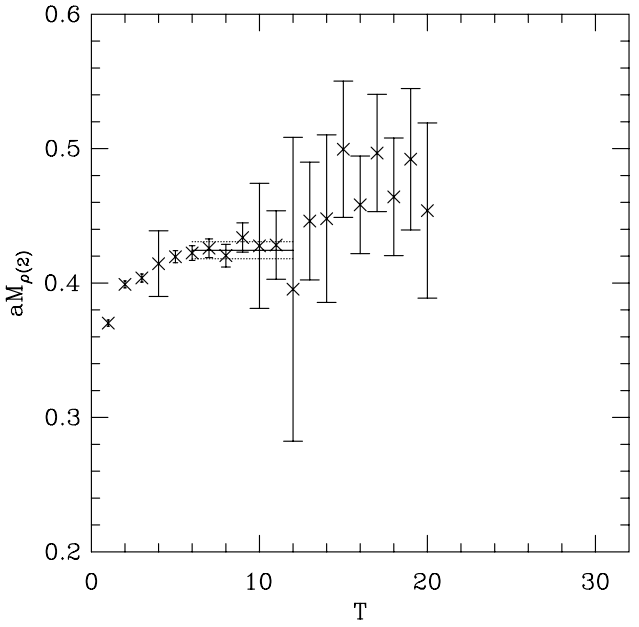

FIG. 1. Effective mass plot of aM_ρ at quark mass 0.01.

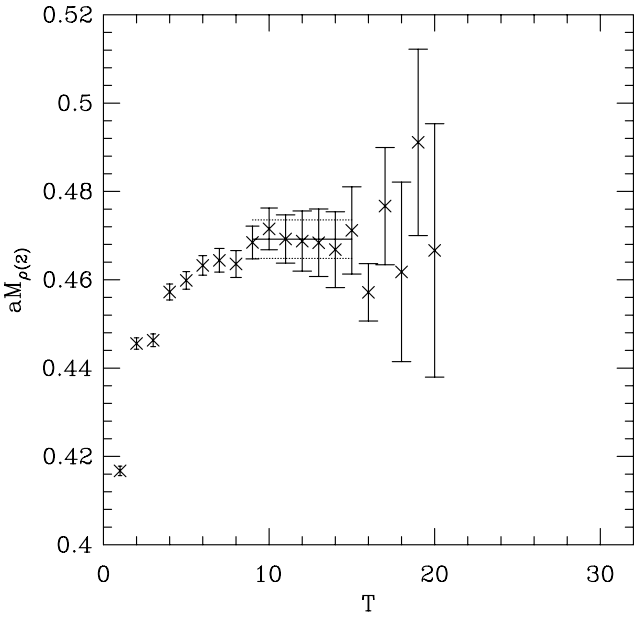

FIG. 3. Effective mass plot of aM_ρ at quark mass 0.03.

$[a(m_u + m_d)/2 \sim 0.0015]$ rather than the chiral limit is smaller than our statistical errors and we do not include it. We also do not include the $m_q^{1/2}$ and $m_q^{3/2}$ terms from pion loops [14] in our chiral fit, as they are expected to have small coefficients, and we have too few mass points to reliably include them.

A potential problem with our estimate of the scale is our use of a relatively small volume ($L \approx 1.6$ fm). Although we expect this is large enough to study kaon properties (since $m_K L \approx 5$ is larger than the range 3–4 where significant effects usually set in), we are relying in our scale determination on results from all four quark masses. At the lightest quark mass $M_\pi L = 2.7$, and volume errors may be significant. Evidence that this is the case comes from Ref. [11], who have results for M_ρ for three different volumes at $\beta = 6$. The finite volume effects can be seen from the resulting estimates of the scale: $1/a = 1.87(6)$, 1.88(4) and 2.01(2) GeV, for 18^3, 24^3 and 32^3 lattices, respectively. Thus we may have underestimated the scale by $\approx 7\%$. It turns out, however, that this uncertainty is smaller than the range of scales resulting from the use of

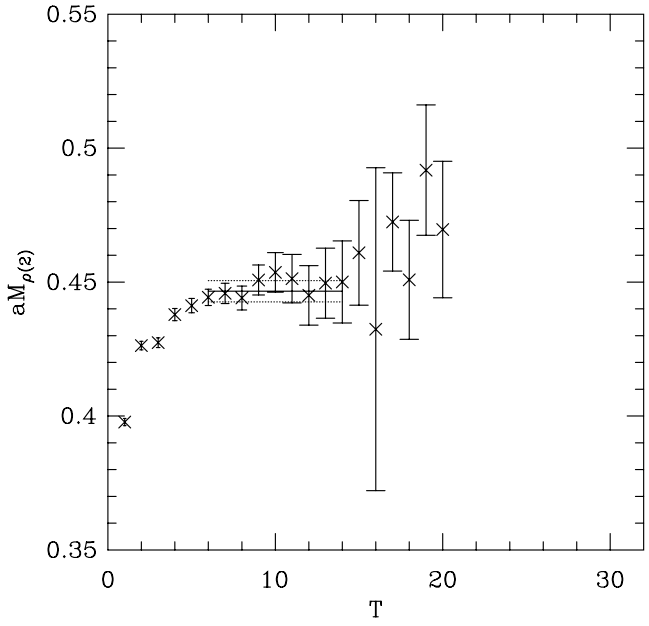

FIG. 2. Effective mass plot of aM_ρ at quark mass 0.02.

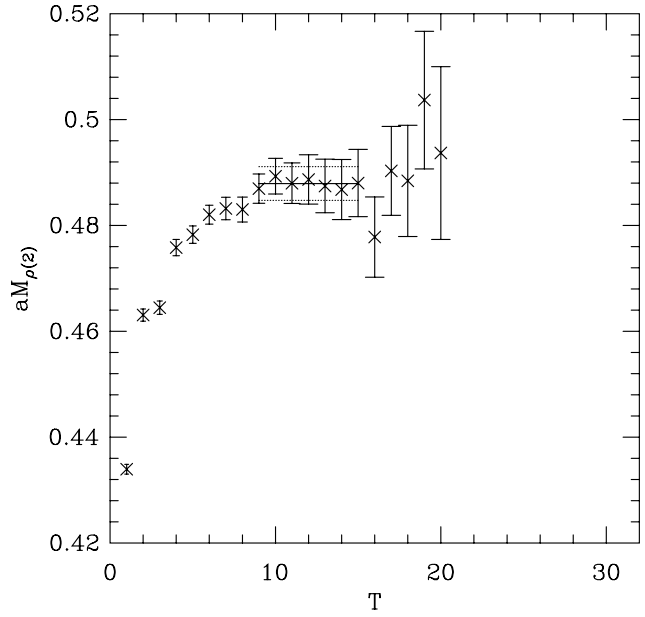

FIG. 4. Effective mass plot of aM_ρ at quark mass 0.04.

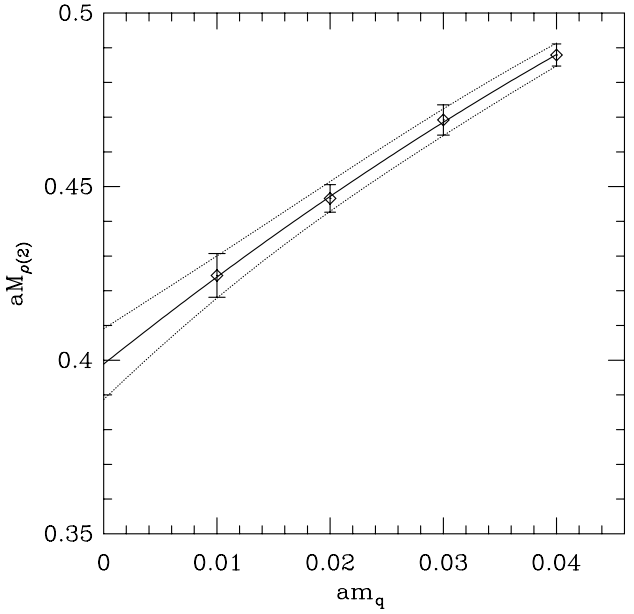

FIG. 5. aM_ρ vs quark mass.

different physical quantities, and so can be subsumed into the quenching error discussed below.

Data for the a_1 meson have much larger errors and we use a simple linear fit. The result, shown in Fig. 6, gives

$$aM_{a_1} = 0.58(4) + 2.1(1.0)(am_q). \quad (4)$$

Again, the chirally extrapolated value is used to determine the estimate of $1/a$ given in Table II.

One of the well-known uncertainties introduced by quenching is that different physical quantities lead to different values of the lattice spacing. Since we are interested here in comparing with other quenched results for m_s and B_K, we follow most previous calculations and determine our central value for the scale, $1/a = 1.95$ GeV, using ρ masses. This lies within the range of values quoted above from the JLQCD B_K calculation, and is close to the value, $1/a = 1.855(38)$ GeV, they use when estimating m_s [10]. Nevertheless, to understand the impact of the scale uncertainty, and, as noted above, to include possible finite volume errors, we also analyze subsequent data using $1/a = 2.1$ GeV. This value is consistent with our estimate from a_1 as well as the result obtained using the Sommer parameter r_0 [15] ($1/a = 2.12$ GeV). The latter is derived from the static $q\overline{q}$ potential and thus is independent of the fermion action.

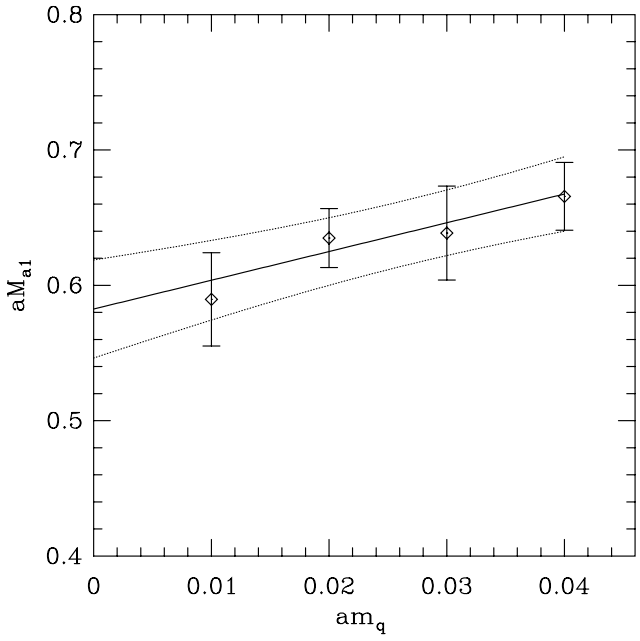

FIG. 6. aM_{a1} vs quark mass.

III. STRANGE QUARK MASS

Our results for the masses of the lattice psuedo-Goldstone pion (spin taste $\gamma_5 \otimes \xi_5$) are presented in Table III. The results with different sources and sinks are consistent, and we use the weighted average of the four results in the subsequent analysis.

The strange quark mass m_s is determined by requiring a fictitious $\bar{s}s$ pseudoscalar mass to match the physical value of $(2M_K^2 - M_\pi^2)$ which corresponds to $(aM_{PS})^2 = 0.1234$ with $1/a = 1.95$ GeV. A linear fit for $(aM_{PS})^2$ versus am_q works well, as shown in Fig. 7. This fit gives $am_s = 0.0520(7)$, and thus $m_s = 102(1.3)$ MeV. Repeating the analysis with $1/a = 2.1$ GeV leads instead to 110(1.5) MeV. We stress that these results are not very sensitive to the chiral fit form used. For example, a fit that includes a quenched chiral logarithm [16,17] and is forced to pass through the origin reduces m_s by 2.1(6) MeV. Such consistency is not surprising since $am_s = 0.052$ is larger than the simulated points, whereas quenched chiral logarithms are important only at masses smaller than $am_q = 0.01$.

As discussed in the previous section, we expect that finite volume effects should be small in our determination of m_s, because our heaviest two quark masses dominate the determination, and these have relatively large values of $M_\pi L$, 4.3 and 5.0, respectively. According to the quenched chiral perturbation theory analysis of Ref. [17], one would expect M_π^2 to be larger than its infinite volume value by 1%–2% in this quark mass range. This would lead to our

TABLE III. Pion masses using axial and pseudoscalar operators from left ($t = 10$) and right ($t = 36$) wall sources.

m_q	$aM_\pi(A_4, L)$	$aM_\pi(A_4, R)$	$aM_\pi(P, L)$	$aM_\pi(P, R)$
m_1	0.1697(29)	0.1682(30)	0.1658(50)	0.1644(56)
m_2	0.2266(27)	0.2255(28)	0.2248(40)	0.2224(42)
m_3	0.2732(27)	0.2725(26)	0.2716(35)	0.2695(34)
m_4	0.3136(27)	0.3134(24)	0.3120(32)	0.3106(30)

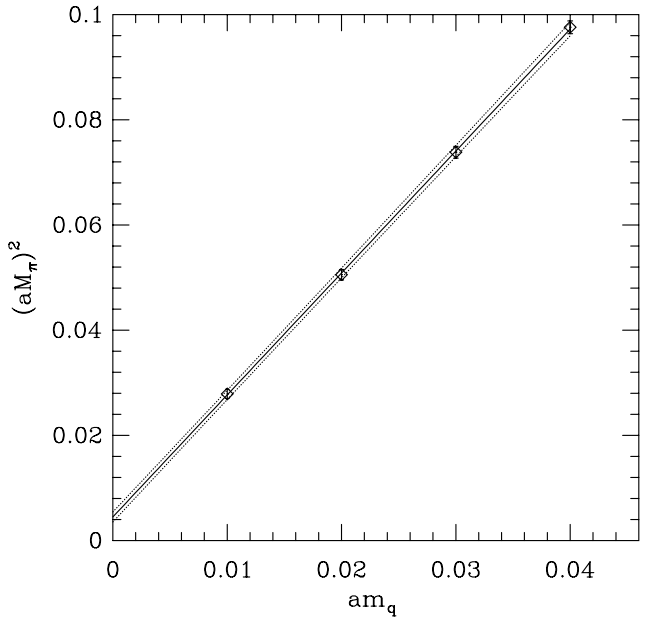

FIG. 7. $(aM_\pi)^2$ vs quark mass.

finite volume result for m_s being 1%–2% smaller than the infinite volume value. This estimate assumes the quenched hairpin parameter to be $\delta \approx 0.2$; using more recent values of $\delta \approx 0.1$ reduces the effect proportionally. That the finite size effects are no larger than this size is supported by the numerical analysis of finite volume effects given in Ref. [18].

Finite volume errors also enter into our result for m_s through their effect on the scale, as discussed in the previous section. We choose, however, to quote a value for m_s for a definite choice of scale, so as to allow a more straightforward comparison with other results. In particular, using the one-loop matching factor from Ref. [6], and the scale $1/a = 1.95$ GeV, we find the renormalized mass $m_s(\overline{\text{MS}}, 2\text{ GeV}) = 101.2 \pm 1.3 \pm 4$ MeV. Here the first error is statistical, while the second is from the systematic effects that we control aside from the scale uncertainty. It is dominated by the uncertainty in Z_m, which we estimate as 4% by assuming a two-loop term of size $\pm 1 \times (\alpha_s)^2$. It also contains the uncertainty from the form of chiral fit used, and from the finite volume errors in M_π^2 discussed in the previous paragraph. Note that we take the central value from the fit form without quenched chiral logarithms so as to better compare to the results of Ref. [10].

This result for m_s allows us to study the efficacy of HYP improved staggered fermions. The state-of-the-art quenched estimate for unimproved staggered quarks (obtained using the same definition of m_s, and $M_{\rho(1)}$ for setting the scale) is $m_s(\overline{\text{MS}}, 2\text{ GeV}) = 106.0 \pm 7.1$ MeV, after extrapolation to the continuum limit [10]. Our first observation is that our result at $\beta = 6.0$ agrees with this continuum value, consistent with our expectation that a^2 errors should not be large. In this respect, we note that it was necessary to go down to lattice spacing $a = 0.06$ fm with unimproved staggered fermions in order to obtain the continuum estimate [10].

It is also useful to compare with the results from Ref. [10] obtained at our coupling, $\beta = 6$. Their bare quark mass, $am_s = 0.0244$ or $m_s = 45$ MeV, is much smaller than ours. Using nonperturbative renormalization they find $m_s(\overline{\text{MS}}, 2\text{ GeV}) = 114$ MeV. The very large matching factor, $Z_m \approx 2.5$, shows the need for nonperturbative renormalization with unimproved staggered fermions. Indeed, using one-loop matching they find the significantly smaller value $m_s(\overline{\text{MS}}, 2\text{ GeV}) = 84$ MeV. By contrast, our matching factor is very close to unity, illustrating one of the advantages of HYP smeared staggered fermions.

Quantifying improvement in discretization errors is more difficult. The unimproved (but nonperturbatively renormalized) result drops by 8 MeV between $\beta = 6$ and the continuum, whereas our result is 5 MeV lower than the continuum value. Since these differences are comparable to the errors, the only definite conclusion we can draw is that the discretization errors appear to not be worsened by improvement.[3]

IV. B_K

The ratio of correlators corresponding to Eq. (1) is measured on the interval $1 \le t \le 25$ between two random U(1) sources [19] placed at $t = 0$ and 26. We find that the individual pseudoscalar meson correlators exhibit contamination from excited states up to ≈ 9 time slices from the sources. For this reason we choose to make constant fits to the central part of the plateau on time slices $9 \le t \le 16$ even though the estimate is stable over the range $4 \le t \le 20$. These fits are shown in Figs. 8–11. In the first column of Table IV we give the resulting bare values for B_K, i.e. with all renormalization constants set to unity, for each of the quark masses. In the second column we give the results after renormalization to the $\overline{\text{MS}}$, naive dimensional regularization (NDR) scheme at scale $\mu = 1/a$.

To quote results in the $\overline{\text{MS}}$ scheme we use the one-loop renormalization factors of Ref. [9], with the matching scale chosen to be $q^* = 1/a$. The coupling $\alpha_s(q^* = 1/a) = 0.192$ is calculated from the plaquette expectation value ($P = 0.593\,67$) using the method of Ref. [20]. At the physical kaon mass, which corresponds to $am_q = 0.026$, the one-loop corrections lead to a $\sim$10% change in B_K. This is very similar to the corresponding shift with unimproved staggered fermions.

To extract B_K at the physical kaon mass we fit the data to the form predicted by quenched chiral perturbation theory including finite volume corrections [17]

[3]This conclusion is bolstered by the fact that Ref. [10] uses a smaller scale than us (1.85 rather than 1.95 GeV). Had they used the larger scale, their final result at $\beta = 6$ would have differed more from the continuum value.

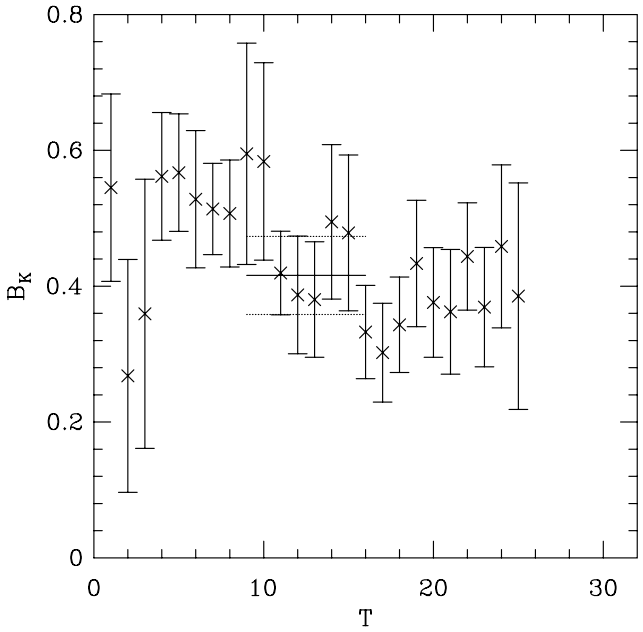

FIG. 8. B_K at quark mass 0.01.

$$B_K = b_0\Big\{1 - 6.0\frac{M_K^2}{(4\pi f)^2}\log\Big[\frac{M_K^2}{(4\pi f)^2}\Big] + \frac{2}{f^2}[-2g_1(M_K^2, 0, L) + M_K^2 g_2(M_K^2, 0, L)]\Big\} + b_1 M_K^2 + b_2 M_K^4, \quad (5)$$

where f is the decay constant, which we fix to 132 MeV. The finite volume dependence enters through the functions g_i, defined in Ref. [21]. This dependence of B_K(NDR, $\mu = 1/a$) on the quark mass is shown by the solid line in Fig. 12 with parameter values $b_0 = 0.23(9)$, $b_1 = 0.5(1.1)/\mathrm{GeV}^2$ and $b_2 = -1.2(1.3)/\mathrm{GeV}^4$. Since the prediction for the finite volume corrections becomes unreliable once $M_K L$ becomes small, we do not display the fit function below $M_K L = 2$.

Our results are consistent with the curvature predicted by the chiral logarithm in Eq. (5). Indeed, we can set $b_2 = 0$ and obtain a good fit [with $b_0 = 0.283(29)$ and $b_1 = -0.30(19)\ \mathrm{GeV}^{-2}$], showing that the curvature can be accounted for by the logarithm alone. Another consistency

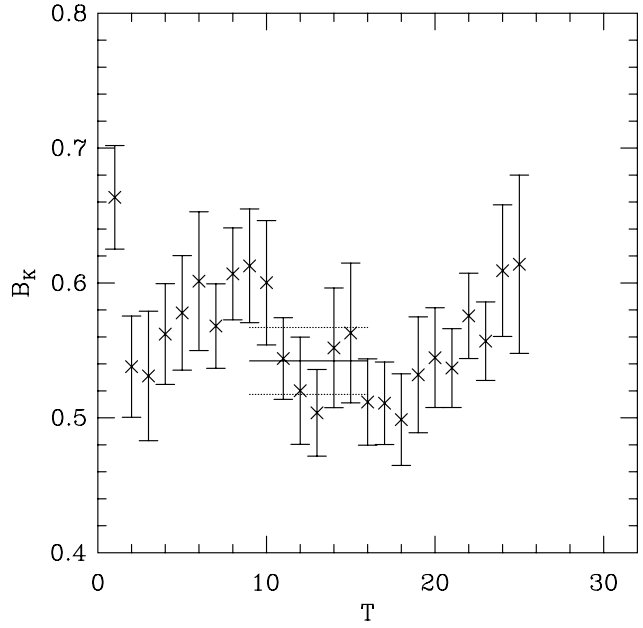

FIG. 9. B_K at quark mass 0.02.

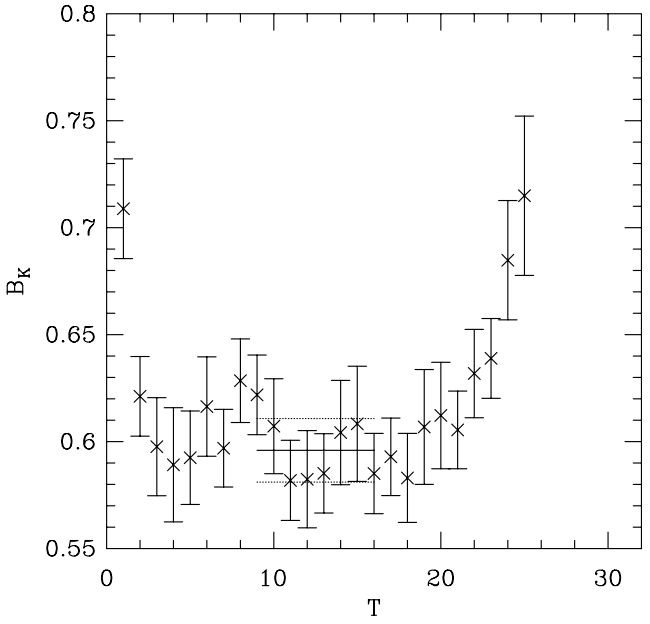

FIG. 10. B_K at quark mass 0.03.

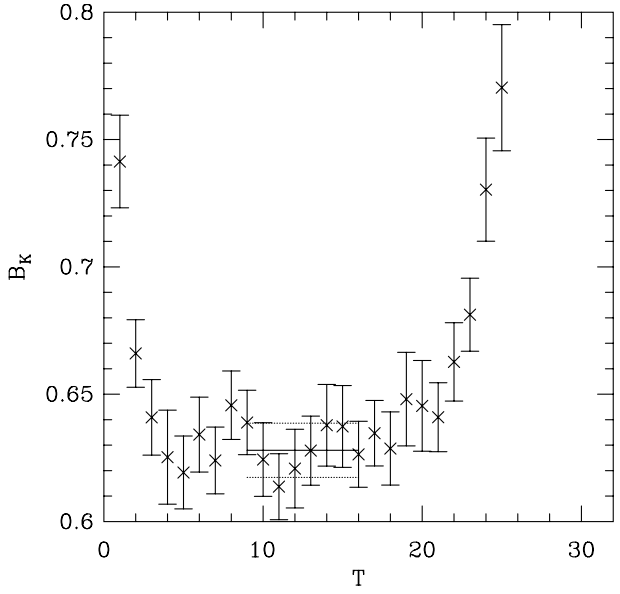

FIG. 11. B_K at quark mass 0.04.

TABLE IV. Results for bare B_K, B_K(NDR, $\mu = 1/a, L$) and estimate of finite volume shift: $\delta B_K(L) = B_K(L = \infty) - B_K(L)$. Errors are statistical.

m_q	Bare B_K	$B_K(1/a, L)$	$\delta B_K(1/a, L)$
m_1	0.514(61)	0.416(57)	+0.0094(38)
m_2	0.614(26)	0.542(25)	+0.0013(5)
m_3	0.658(16)	0.596(15)	−0.0003(1)
m_4	0.686(11)	0.628(11)	−0.0006(2)

check is that b_1 and b_2 agree with the expectations of naive dimensional analysis, namely $|b_1| \approx |b_2| \approx 1$ in units of the scale, ~1 GeV, of chiral perturbation theory. Taken as a whole, previous work is inconclusive concerning the presence of the chiral logarithm with predicted coefficient, largely due to the relatively high quark masses used ($m > m_s/2$). It is only by extending the range to $m_s/5$ that we find evidence, albeit not conclusive, for the onset of the expected chiral logarithm at small quark masses.

It is important to obtain a good fit to the chiral behavior in order to reliably extract estimates of finite volume corrections. The smallest value of $M_K L$ is 2.64, so one expects such corrections to be large [22]. For B_K, however, the cancellation between g_1 and g_2 terms suppresses these corrections. Based on our chiral fit, the third column in Table IV gives estimates for this finite volume shift. Note that the correction is nonmonotonic in M_K, due to the cancellation noted above. The infinite volume prediction is shown in Fig. 12. From this we conclude that for physical M_K the finite volume shift in B_K is much smaller than quoted errors even on our small lattices. This conclusion is supported by the absence of finite volume errors in the JLQCD results at $\beta = 6$ using unimproved staggered fermions [11].

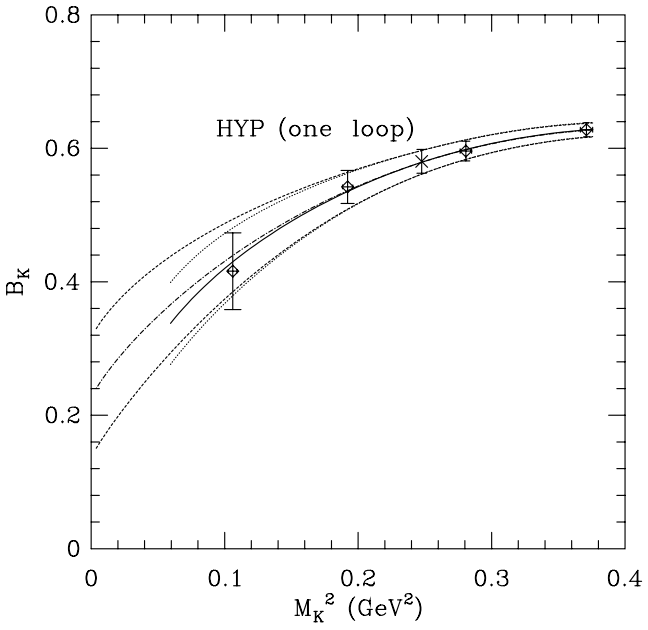

FIG. 12. Results for B_K(NDR, $\mu = 1/a$) (diamonds), fit to the expected chiral form at finite volume (solid line, errors small dashes). The dot-dashed line (errors long dashes) is the corresponding infinite volume result. The cross is the infinite volume result at the physical kaon mass.

Our final results are obtained by evolving from $1/a$ to $\mu = 2$ GeV using the two-loop renormalization group running for $N_f = 0$ [23]. We find

$$B_K(\text{NDR}, 2\ \text{GeV}) = 0.578 \pm 0.018 \pm 0.042, \quad (6)$$

$$B_K^{\text{RGI}} = 0.806 \pm 0.025 \pm 0.058, \quad (7)$$

$$b_0^{\text{RGI}} = 0.314 \pm 0.124 \pm 0.176, \quad (8)$$

where B_K^{RGI} is the renormalization group invariant $B-$ parameter [23], with b_0^{RGI} its value in the chiral limit. The first error combines that from statistics and those due to the chiral interpolation (or extrapolation for b_0). The second is our estimate of the uncertainty from using one-loop matching factors explained below. Aside from the errors due to quenching and the use of degenerate quarks, which we do not address here, other systematics lead to changes smaller than the perturbative error. For example, using the scale from r_0 reduces B_K(NDR, 2 GeV) and b_0^{RGI} by 0.025 and 0.007, respectively, while setting $b_2 = 0$ in the chiral fit increases them by 0.011 and 0.079. If we use $f = f_K = 159.8$ MeV instead of $f = 132$ MeV in Eq. (5) and fit the data, B_K changes by less than 0.01%, while b_0 increases by 5%.

The error associated with unknown α^2 corrections is estimated as follows. We can write $B_K = B_A + B_V$, where V and A refer to vector-vector and axial-axial parts of the operator in Eq. (1). $B_{A,V}$ can each be decomposed into one and two color-trace parts [3]. Each of these four components of B_K is proportional to $\log(M_K^2)$ and thus diverges in the chiral limit, although their sum does not. Using one-loop matching there is an incomplete cancellation, and the resulting B_K should diverge in the chiral limit, although this feature is expected to manifest itself at much smaller quark masses than studied here. Indeed, the bare values for $B_{V,A}$ do indicate a divergent behavior. Because of the residual divergence, we cannot simply estimate the error, in particular, in b_0, by multiplying by an overall relative correction of $\pm\alpha(q^*)^2$ (as we did for m_s). Instead, we recalculate B_K after adding $\pm\alpha(q^*)^2$ to the matching factors for each of the four components of B_K in turn, and take the largest variation as the error. The resulting uncertainty, quoted above, is larger than the statistical error and, as expected, grows rapidly in the chiral limit.

Even though we need more high precision data at lighter quark masses to pin down the chiral extrapolation, it is nevertheless interesting that our estimate $b_0^{\text{RGI}} = 0.314 \pm 0.124 \pm 0.176$ is in good agreement with recent estimates

0.29(15) [24] and 0.36(15) [25] obtained using $1/N_c$ expansion.

We now compare our estimate with the state-of-the-art results obtained by the JLQCD Collaboration [11] using unimproved staggered fermions and argue that HYP smearing reduces discretization errors. The JLQCD result in the continuum limit is $B_K(\mathrm{NDR}, 2\ \mathrm{GeV}) = 0.628 \pm 0.042$. Our first observation is that our result at $\beta = 6$ is consistent with this continuum result. On the one hand, this indicates that the a^2 errors with HYP fermions are not large, as for m_s. On the other hand, the value of B_K at $\beta = 6$ with unimproved staggered fermions [0.679(2)] is also consistent with the continuum result, giving no evidence of improvement.

We can go further, however, using the details of the continuum extrapolation provided by Ref. [11]. Their fit included both a^2 and α_s^2 terms. Using their fit parameters we can determine two additional estimates of B_K at $\beta = 6.0$: removing only the $O(\alpha^2)$ term [and not the $O(a^2)$ discretization correction] and vice versa. The original results and those corrected for either the discretization or perturbative errors alone are given in Table V. The point we wish to make is that in the case of gauge-invariant operators (which are those we use) the JLQCD fits imply that, at $\beta = 6$, the total result 0.68 contains an $O(a^2)$ contribution of ~ 0.13 and an $O(\alpha^2)$ contribution of ~ -0.08. (Corrections for non-gauge-invariant operators, which are not the operators of choice, are somewhat smaller but show the same pattern.) Thus, in a formulation where only discretization errors were eliminated or substantially reduced one should expect a final result closer to 0.55 at $a \approx 0.1$ fermi. Our estimate with HYP smearing, $B_K(\mathrm{NDR}, 2\ \mathrm{GeV}) = 0.58(4)$, is indeed consistent with this and significantly different from the unimproved JLQCD result 0.679(2). This suggests that discretization errors have been reduced by using HYP smeared fermions.

This conclusion is supported by the fact that all calculations with domain wall or overlap fermions, which are also expected to have small discretization errors and small perturbative corrections, find values at $\beta = 6$ consistent with ours: 0.575(6) (Ref. [26]), 0.532(11) (Ref. [27]), 0.563(31) (mean of data at $\beta = 5.9$ and 6.1 in Ref. [28]), and 0.63(6) (Ref. [29]). Here, only statistical errors have been quoted.

Finally, we consider the results in Table V with "α^2 removed." These correspond approximately to using nonperturbative matching factors, and should thus expose the "true" a^2 errors in the unimproved results. Unfortunately, the large errors preclude definitive conclusions. Nevertheless, the fact that our result 0.58(4) differs from the α^2 removed unimproved result of 0.76(6) by about 2σ, while lying closer to the continuum result 0.62(4), is consistent with our conclusion that discretization errors are reduced by using smeared links.

TABLE V. $B_K(\mathrm{NDR}, 2\ \mathrm{GeV})$ at $\beta = 6$ for gauge-invariant (GI) and noninvariant (NGI) operators, before and after removing the fitted a^2 and α^2 terms. Data from Ref. [11].

Type	Uncorrected	a^2 removed	α^2 removed
GI	0.6790(16)	0.55(7)	0.76(7)
NGI	0.7128(14)	0.61(7)	0.73(7)

V. CONCLUSION

We conclude that improved staggered fermions are a viable and promising option for calculations of m_s and B_K in full QCD simulations. The difficulties observed with unimproved staggered fermions (ill behaved perturbation theory for Z_m in the case of m_s and discretization errors in B_K) are greatly reduced. Our study suggests that reliable calculations should be possible on the ensembles of lattices being generated with dynamical improved staggered fermions without requiring very small lattice spacings. There are two caveats, however. To reduce the uncertainty due to the two-loop term in the renormalization constants below our estimates of 4% in m_s and 7% in B_K will require a demanding two-loop or nonperturbative calculation of matching factors and the calculation of a larger set of lattice matrix elements. Second, in the case of B_K, the estimate in the chiral limit is very sensitive to errors in the matching factors, as well as to the chiral extrapolation.

ACKNOWLEDGMENTS

This calculation has been done on the Columbia QCDSP supercomputer. We thank N. Christ, C. Jung, C. Kim, G. Liu, R. Mawhinney and L. Wu for their support on this staggered ϵ'/ϵ project. This work is supported in part by BK21, by the Interdisciplinary Research Grant of Seoul National University and by KOSEF Contract No. R01-2003-000-10229-0, the US-DOE Grant No. KA-04-01010-E161 and Contract No. DE-FG02-96ER40956. We gratefully acknowledge discussions with A. Soni.

[1] D. Becirevic, Nucl. Phys. B, Proc. Suppl. **129/130**, 34 (2004).
[2] C. T. H. Davies *et al.*, Phys. Rev. Lett. **92**, 022001 (2004).
[3] G. Kilcup, R. Gupta, and S. R. Sharpe, Phys. Rev. D **57**, 1654 (1998).
[4] M. Golterman, Nucl. Phys. B, Proc. Suppl. **73**, 906 (1999).

[5] J. F. Lagae and D. K. Sinclair, Phys. Rev. D **59**, 014511 (1999); G. P. Lepage, *ibid.* **59**, 074502 (1999).
[6] W. Lee and S. Sharpe, Phys. Rev. D **66**, 114501 (2002).
[7] A. Hasenfratz and F. Knechtli, Phys. Rev. D **64**, 034504 (2001).
[8] MILC Collaboration, K. Orginos and D. Toussaint, Phys. Rev. D **59**, 014501 (1999).
[9] W. Lee and S. Sharpe, Phys. Rev. D **68**, 054510 (2003).
[10] S. Aoki *et al.*, Phys. Rev. Lett. **82**, 4392 (1999).
[11] S. Aoki *et al.*, Phys. Rev. Lett. **80**, 5271 (1998).
[12] C. Sui, Ph.D. thesis, Columbia University, 2000.
[13] M. F. Golterman, Nucl. Phys. **B273**, 663 (1986).
[14] M. Booth, G. Chiladze, and A. F. Falk, Phys. Rev. D **55**, 3092 (1997).
[15] R. Sommer, Nucl. Phys. **B411**, 839 (1994).
[16] C. W. Bernard and M. F. L. Golterman, Phys. Rev. D **46**, 853 (1992).
[17] S. Sharpe, Phys. Rev. D **46**, 3146 (1992).
[18] S. Aoki *et al.*, Phys. Rev. D **50**, 486 (1994).
[19] D. Pekurovsky and G. Kilcup, Phys. Rev. D **64**, 074502 (2001).
[20] C. T. H. Davies *et al.*, Phys. Rev. D **56**, 2755 (1997).
[21] J. Gasser and H. Leutwyler, Phys. Lett. B **184**, 83 (1987); **188**, 477 (1987).
[22] D. Becirevic and G. Villadoro, Phys. Rev. D **69**, 054010 (2004).
[23] J. Buras, M. Jamin, and P. Weisz, Nucl. Phys. **B347**, 491 (1990).
[24] J. Prades, J. Bijnens, and E. Gamiz, hep-ph/0501177.
[25] O. Cata and S. Peris, J. High Energy Phys. 03 (2003) 060.
[26] A. Ali Khan *et al.*, Phys. Rev. D **64**, 114506 (2001).
[27] RBC Collaboration, T. Blum *et al.*, Phys. Rev. D **68**, 114506 (2003).
[28] Thomas DeGrand, Phys. Rev. D **69**, 014504 (2004).
[29] Nicolas Garron *et al.*, Phys. Rev. Lett. **92**, 042001 (2004).